ADVANCED QUANTUM TECHNOLOGIES
www.advquantumtech.com

Experimental Realization of Parrondo's Paradox in 1D Quantum Walks

Munsif Jan, Qin-Qin Wang, Xiao-Ye Xu, Wei-Wei Pan, Zhe Chen, Yong-Jian Han,* Chuan-Feng Li,* Guang-Can Guo, and Derek Abbott*

The Parrondo effect is a well-known apparent paradox where a combination of biased random walks displays a counterintuitive reversal in direction. These random walks can be expressed in terms of classical coin tossing games, leading to the surprising result that a combination of losing games can result in a winning game. There is now a large body of literature on quantum walks theoretically analyzing the quantum version of this effect, but to date, there have been no experimental observations of quantum Parrondo walks. Here, the first experimental verification of a quantum Parrondo walk within a quantum optics scenario is demonstrated. Based on the compact large-scale experimental quantum-walk platform, two rotation operators are implemented to realize the quantum Parrondo effect. The effect of quantum coherence in a quantum Parrondo walk is also investigated based on a delayed-choice scheme that cannot be realized with classical light. It is demonstrated that the Parrondo effect vanishes when the quantum walk has a completely decoherent initial state in a delayed-choice setting. Quantum walks are fundamental to multiple quantum algorithms, and this research provides motivation to expand the results to further explore quantum Parrondo walks.

1. Introduction

Parrondo's paradox was introduced through the analysis of the flashing Brownian ratchet,[1,2] and describes a counterintuitive result of combining two individually losing games to produce a winning outcome.[3,4] Parrondo's paradox received significant interest, and has impacted several fields, including physics,[5–13] population genetics,[14–16] and economics[17] since its appearance as it provides the mathematical framework for describing the strategy of turning unfavorable scenarios into favorable ones. Within a physical context, the Parrondo effect demonstrates how mixing dynamical processes can result in a surprising reversal in dynamics. Though applications of the Parrondo effect have been proposed in classical and quantum systems,[5,6,11–13,18] to the best of our knowledge, the experimental realization of a quantum version of the effect has remained an unsolved challenge. The classical Parrondo effect is a well-known type of random walk that can be described by the Fokker-Planck equation.[19] Because the Fokker–Planck equation is also a Wick rotation of the Schrödinger equation,[20] there exist deep interconnections between these types of random and quantum walks. Our work motivates the future exploration of these ideas.

Quantum walks (QWs)[21,22] are a natural extension of classical random walks (CRWs) in the quantum domain, that offer a flexible and powerful platform for the investigation of physical phenomena, ranging from the design of efficient algorithms in quantum information processing[23–25] (even constructing universal quantum computation[26,27]) and the realization of exotic physical phenomena in the context topological phases[28–30] to quantum physics out of equilibrium[31] (for example, observing the dynamical quantum phase transition[32–34] and investigating quantum thermodynamics[35–39]). Recently, an experiment to investigate the quantum nature of the distinct behaviors of QWs was proposed and demonstrated using a delayed-choice method.[40]

Quantum walks exhibiting the Parrondo effect have been proposed and theoretically analyzed.[41–44] Quantum Parrondo games are a special case of QWs in an environment with disorder.[45,46] These disordered QWs randomly choose a coin-tossing operation from a given set at each step, and feature distinctive properties, such as enhanced entanglement.[47–49] Unlike the CRWs, QWs are characterized by quantum superpositions of amplitudes instead of classical probability distributions. The coherent character of the QW plays a key role in the realization of a quantum Parrondo game by producing a correlation between two individually losing games when they are played in alternation, which is the most important ingredient for the occurrence

Dr. M. Jan, Dr. Q.-Q. Wang, Prof. X.-Y. Xu, Dr. W.-W. Pan, Z. Chen, Prof. Y.-J. Han, Prof. C.-F. Li, Prof. G.-C. Guo
CAS Key Laboratory of Quantum Information
University of Science and Technology of China
Hefei 230026, P. R. China
E-mail: xuxiaoye@ustc.edu.cn; smhan@ustc.edu.cn; cfli@ustc.edu.cn
Dr. M. Jan, Dr. Q.-Q. Wang, Prof. X.-Y. Xu, Dr. W.-W. Pan, Z. Chen, Prof. Y.-J. Han, Prof. C.-F. Li, Prof. G.-C. Guo
CAS Center for Excellence in Quantum Information and Quantum Physics
University of Science and Technology of China
Hefei 230026, P. R. China
Prof. D. Abbott
School of Electrical and Electronic Engineering
The University of Adelaide
SA 5005, Australia

The ORCID identification number(s) for the author(s) of this article can be found under https://doi.org/10.1002/qute.201900127

DOI: 10.1002/qute.201900127

of Parrondo effects.[6] The main challenge for an experimental demonstration of a quantum Parrondo game is that the QW must be accurately manipulated with a large number of steps.

Based on our recently developed compact large-scale QW platform,[50] we demonstrate the quantum Parrondo effect with the following process. QWs with different coin operations, that is, R_A and R_B, are labeled as games A and B, respectively. We show that these games are individually losing games, but when they are alternated in an ABB sequence, they become a winning game, which is the counterintuitive reversal known as Parrondo's paradox. In addition, we also experimentally demonstrate the impact of quantum coherence on the Parrondo effect by showing that it vanishes when the QW has a completely decoherent initial state in a delayed-choice setting, indicating that quantum coherence plays a critical role in the appearance of the Parrondo effect.

2. Theoretical Background

We consider 1D discrete-time QWs with a total Hilbert space can be expressed as $H = H_c \otimes H_p$, where H_c is a 2D coin space spanned by $\{|0\rangle, |1\rangle\}$, and H_p represents an infinite-dimensional site space spanned by $|x\rangle$ ($x \in Z$ is the site). Each step of the QW possesses two operations of R, the rotation of the coin state in H_C, and S, the shift operator that describes the movement of a walker according to the coin state. Generally, the rotation operator for a 2D space is defined by three parameters α, β, and γ, that is,

$$R(\alpha, \beta, \gamma) = \begin{pmatrix} e^{i\alpha}\cos\beta & -e^{-i\gamma}\sin\beta \\ e^{i\gamma}\sin\beta & e^{-i\alpha}\cos\beta \end{pmatrix}. \quad (1)$$

Different rotation operators characterize different QWs, so are considered as different games. The shift operator is defined as $S = \sum_{x=-\infty}^{\infty}(|0\rangle\langle 0| \otimes |x+1\rangle_p\langle x|_p + |1\rangle\langle 1| \otimes |x-1\rangle_p\langle x|_p)$, and the one step in the evolution of the QW is described by $U = S{\cdot}R(\alpha, \beta, \gamma)$. In our experiments, the generic unbiased initial state of the walker is prepared as $|\Psi(0)\rangle = \frac{1}{\sqrt{2}}(|0\rangle - i|1\rangle)_c \otimes |x\rangle_p$. The global state at step t (t is an integer) then is expressed as $|\Psi(t)\rangle = U^t|\Psi(0)\rangle$.

To demonstrate the paradoxical scenario of Parrondo's game in a 1D discrete-time QW, we define a game on the state $\Psi(t)$. The bias of the probability distribution of $\Psi(t)$ is used to specify the winning and losing outcomes of the game. The winning and losing regions are shown in **Figure 1**. If $P_R - P_L > 0$ ($P_L = \sum_{x=-\infty}^{-1}|\langle x|\Psi(t)\rangle|^2$ and $P_R = \sum_{x=1}^{\infty}|\langle x|\Psi(t)\rangle|^2$), then the walker has a greater probability of appearing to the right of the origin and represents a winning game. Conversely, if $P_R - P_L < 0$, then the game is losing, and when $P_R = P_L$, the game is a draw. If $P_R - P_L > 0$ is maintained, then a winning expectation is indicated. Similarly, this converse situation denotes a losing expectation, as shown in Figure 1.

We define $P_R - P_L$ as a function of the coin parameters and apply a classical algorithm to search the parameter space to find the subset that displays the Parrondo effect. As an example, we play game A and game B with coin rotation operator $R_A = R(137.2, 29.4, 52.1)$ (orange) and $R_B = R(149.6, 67.4, 132.5)$ (dark grey) set to be in the paradoxical subset, as shown in **Figure 2a**, respectively. Here, $R_{A(B)}$ can change the self-interference pattern of the walker[40] providing constructive interference during its left-biased motion when we play games A and B individually or a constructive interference during its right-biased motion when we play these two games alternating in an ABB sequence (in other words, R_A is applied once and R_B twice at each step) as shown on the right side of Figure 2a. This is thus a demonstration of the Parrondo effect. Here we select the QWs with a period of three rather than two-period QWs.[51–53] This is because for two-period QWs the probability difference is the same as the value obtained from the game A or game B and no Parrondo effect exists.[54]

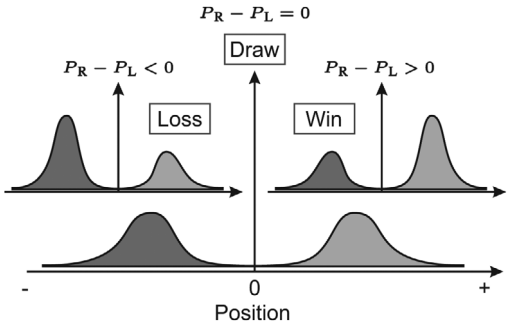

Figure 1. An illustration of a winning versus losing strategy in a 1D QW. Black and grey distributions represent the probabilities of the walker to the left P_L and right P_R of the origin, respectively.

3. Experimental Realization

The layout of the QW experimental setup is shown in Figure 2b. An ultra-fast pulsed laser (Ti:Sapphire, Mira 800) centered at 800 nm with a 76 MHz repetition rate and a 140 fs pulse width was focused on a 2 mm thick beta-barium borate crystal (BBO1) via lens L1 that produced a frequency-doubled ultraviolet pulse centered at 400 nm. Then, the 100 mW ultraviolet pulse split by a dichroic mirror (DM) was focused by lens L3 to pump BBO2, and entangled photon pairs were generated from a type-II non-degenerate beam-like spontaneous parametric down-conversion (SPDC) (for the standard single-particle QW, the "sandwich-like" BBOs was replaced with a single piece of BBO).[55] The signal photons centered at 780 nm represented the walker, and the polarization as the coin with a correspondence $H(V) \leftrightarrow 0(1)$, where $H(V)$ is the horizontal (vertical) polarization of the photon (walker). The idler photons were sent as a trigger into a 7.5 m delay line followed by a projection measurement. The QWs were realized through wave plates and calcite crystals, where a half-wave plate (HWP) and a quarter-wave plate (QWP) implemented the coin toss action, and a birefringent crystal (calcite with length 8.98 mm) implemented the conditional shift (5 ps shift for each step QW). Thus, the arrival time of the signal photons corresponded to the position space. Analyzing the signal photon pulse train with a time interval of approximately 5 ps was challenging for commercial single photon detectors with time resolution typically in the range of tens to hundreds picoseconds.[56] Therefore, an up-converted single-photon detector comprising frequency upconversion with a photomultiplier tube (PMT) was employed because of its high temporal resolution. After projecting the local state on the two bases ($|H\rangle\langle H|$ and $|V\rangle\langle V|$), the number

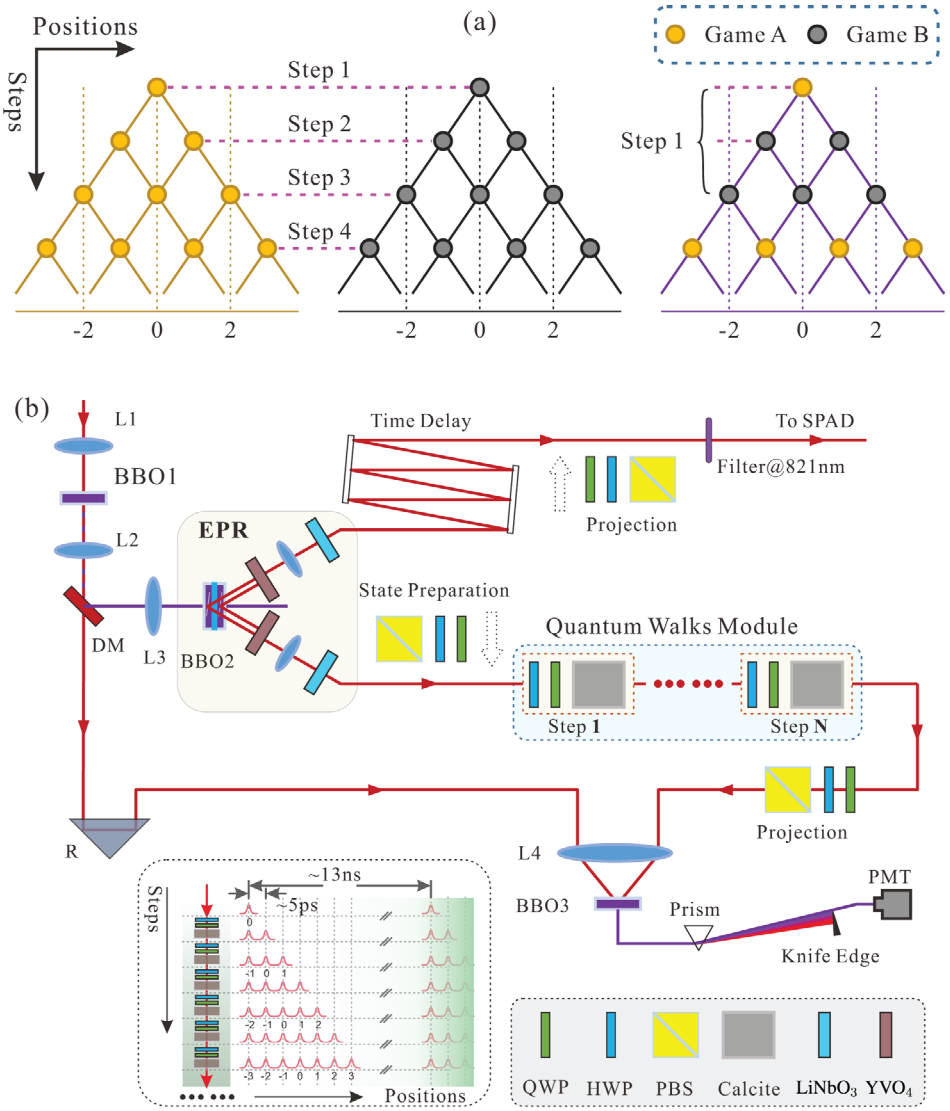

Figure 2. a) An illustration of different game strategies. From left to right, game A realized with R_A (orange), game B realized with R_B (dark grey), and game ABB realized with both coins alternated in the sequence of $R_A R_B R_B$. b) The layout of our experimental setup that includes four parts, 1) generation of a frequency-doubled ultraviolet pulse in BBO1 via second-harmonic generation, 2) generation of polarization-entangled photon pairs by using the type-II non-degenerate beam-like SPDC in a "sandwich-like" structure (we replace the "sandwich-like" BBOs with a single piece of BBO for the standard single-particle QW), 3) realization of time-multiplexing QWs utilizing wave plates and birefringent crystals (detailed descriptions are included in the bottom inset), and 4) detection of single photon arrival times through sum-frequency generation with a pump pulse in BBO3. All three BBOs are β-BaB_2O_4 crystals. The following abbreviations represent lens (L), dichroic mirror (DM), polarization dependent beam splitter (PBS), half-wave plate (HWP), quarter-wave plate (QWP), reflector (R), fiber collimator (FC), single mode fiber (SMF), and single-photon avalanche diode (SPAD). Details about the implementation of QWs can be found in ref. [50].

of photons at each site could be measured via the up-converted single-photon detector to obtain the probability. A spectrum filter based on a 4F system was constructed to reduce the scattering noise before the photons entering the PMT.

Every two birefringent crystals could form an interferometer. Their alignment required the process of carefully tilting the latter crystal around its optical axis perpendicular to the experimental table, which led to maximal interference visibility of the interferometer. The process was repeated to align all the crystals in sequence. The interference visibility was greater than 0.996 for each step, and the temperature fluctuation in the environment was controlled within ±0.2 °C for avoiding unexpected temperature-induced phase shifts of the interferometers.

First, the probability distribution dynamics in 1D discrete-time QWs of heralded single photons was investigated. The walker, initially prepared as $(|H\rangle - i|V\rangle)/\sqrt{2}$ by the polarizer composed of PBS-HWP-QWP, coincided with the idler photons without the optical delay path and projection measurement. In game A (B), the quantum state at step t was $|\Psi(t)\rangle_{A(B)} = (S\cdot R_{A(B)})^t|\Psi(0)\rangle$. The experimental results of the bias of the distribution of the states $\Psi_{A(B)}(t)$, that is, $P_R(t) - P_L(t)$ for games A and B are illustrated in

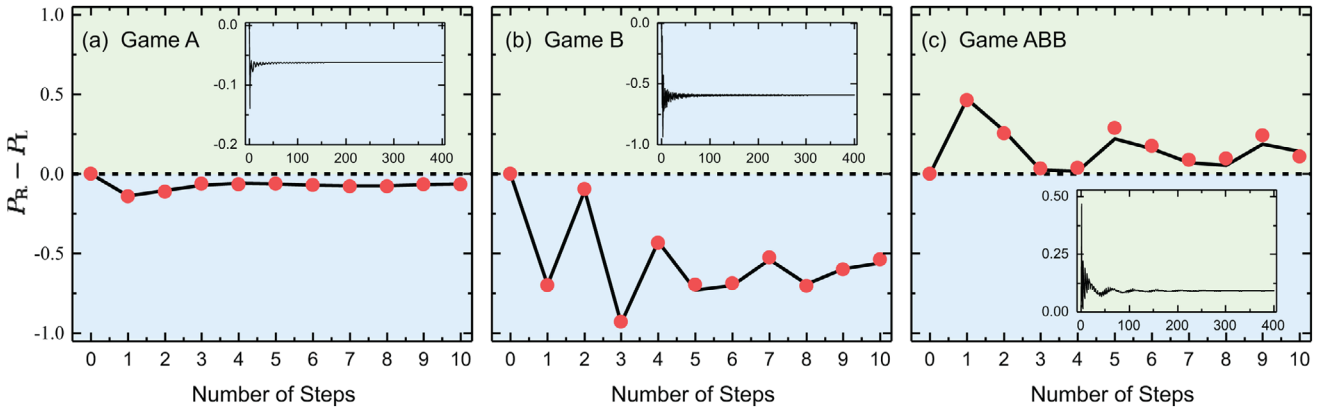

Figure 3. The walker difference probability distribution $P_R - P_L$ for a) game A with coin operation R_A, b) game B with coin operation R_B, c) game ABB with coin operation $R_A R_B R_B$ versus the number of steps. The solid black line and red dots correspond to a short-range simulation and experimental results, while the insets (black lines) display the $P_R - P_L$ long-time dynamics. These demonstrate the occurrence of Parrondo's paradox in 1D discrete-time QWs. Error bars are smaller than the size of the red dots with only consideration of statistical errors.

Figure 3 with Figure 3a corresponding to game A with a rotation operator $R_A = R(137.2, 29.4, 52.1)$, and Figure 3b corresponding to game B with a rotation operator $R_B = R(149.6, 67.4, 132.5)$. Both games A and B were losing games and their bias distributions $P_R - P_L$ were negative up to step 10. The theoretical simulations also showed that these two games would lose for any step t, and are losing for infinite t. Up to step 10, the experimental results agreed with the theoretical results. The similarity, defined as $S = (\sum_x \sqrt{P_{exp}(x)P_{th}(x)})^2$ (P_{exp} and P_{th} are the experimentally measured and theoretical probability distributions, respectively), measures the distance between the experimental and the theoretical results.[57] During the experiment, these values were larger than 0.999 ± 0.001 and 0.992 ± 0.003 for the last step in games A and B, respectively, indicating the high precision of our experiment.

When play of games A and B were alternated by rotating the coins in the sequence of $R_A R_B R_B$ with a period of three, as shown in Figure 2a, some counterintuitive behavior could be observed. In this scenario, the quantum state at step t is $|\Psi(t)\rangle_{ABB} = (S \cdot R_B \cdot S \cdot R_B \cdot S \cdot R_A)^t |\Psi(0)\rangle$, and the experimental results of the bias distribution of the state at any step t are depicted in Figure 3c. While the realization of game ABB required optical elements tripled than game A or B, the similarity of probability distribution for the last step was still higher than 0.909 ± 0.004. This result explicitly showed that $P_R - P_L$ is positive for all the steps up to 10 and the theoretical simulation showed that it will be positive for all steps t. Therefore, according to the definition of losing and winning strategies in the QW, it was demonstrated that the combination of two losing games (A and B) can produce a winning game.

To further show the quantum Parrondo effect in a QW experiment, we performed delayed-choice QWs via entangling the walker to an ancillary photon.[40] In this case, a polarization-entangled two-photon Bell state $|\Phi^+\rangle = (|HH\rangle + |VV\rangle)/\sqrt{2}$ was generated via beam-like SPDC occurring in "sandwich-like" structured BBO crystals labeled as BBO2 in Figure 2b. The signal photon was adopted as the walker and its interference pattern could be delayed-choice via the coin-state projection of the idler photon heralding the walker's state due to the shared quantum entanglement. The delayed-choice coin-state projection was realized by adding a polarization analyzer composed of HWP-QWP-PBS at the idler photon channel, and performed after the walker completes the QWs and was detected at the PMT using the delayed path.

Figure 4 shows the results for delayed-choice QWs. In (a), the idler photon is projected to $(|H\rangle + i|V\rangle)/\sqrt{2}$ while in (b) it is without a special delayed-choice of polarization by moving out the polarizer. The appearance of quantum Parrondo effect is seen in Figure 4a where classical wave mechanics can not explain the results, which is similar to the results of the single-photon scenario as shown from Figure 3. Furthermore, if we destroy the coherence of the coin state, in other words, the walker's coin degenerates to a maximally mixed state, then the counterintuitive phenomenon of the quantum Parrondo effect disappears, as shown by the trivial results in Figure 4b where $P_R - P_L \equiv 0$ for all three cases. The unbiased probability distributions included in the insets of (b) are different from the well-known Gaussian distribution in the classical counterparts, which indicates the quantum coherence still exists in the walker's position space. In other words, the counterintuitive phenomenon is observed again in configuration (a) and its disappearing in (b) indicates that it is intrinsic quantum coherence, rather than its classical counterpart,[58,59] resulting in the quantum Parrondo effect. Any complete decoherence of the coin state or the position space will destroy the counterintuitive effect (the effect of the position space decoherence is discussed in detail in the Appendix).

Quantum entanglement is regarded as a genuine quantum feature with no classical counterpart. The spin-orbit coupling in QWs will result in the generation of entanglement between the internal and external degrees of freedom (defined as coin-position entanglement).[60] Previously, we experimentally demonstrated that dynamic disorder can enhance coin-position entanglement.[49] In this context, the game strategy (ABB) for observing the quantum Parrondo effect can be regarded as a type of disordered QW (within a period three). Further investigation of the entanglement behavior under different conditions involving

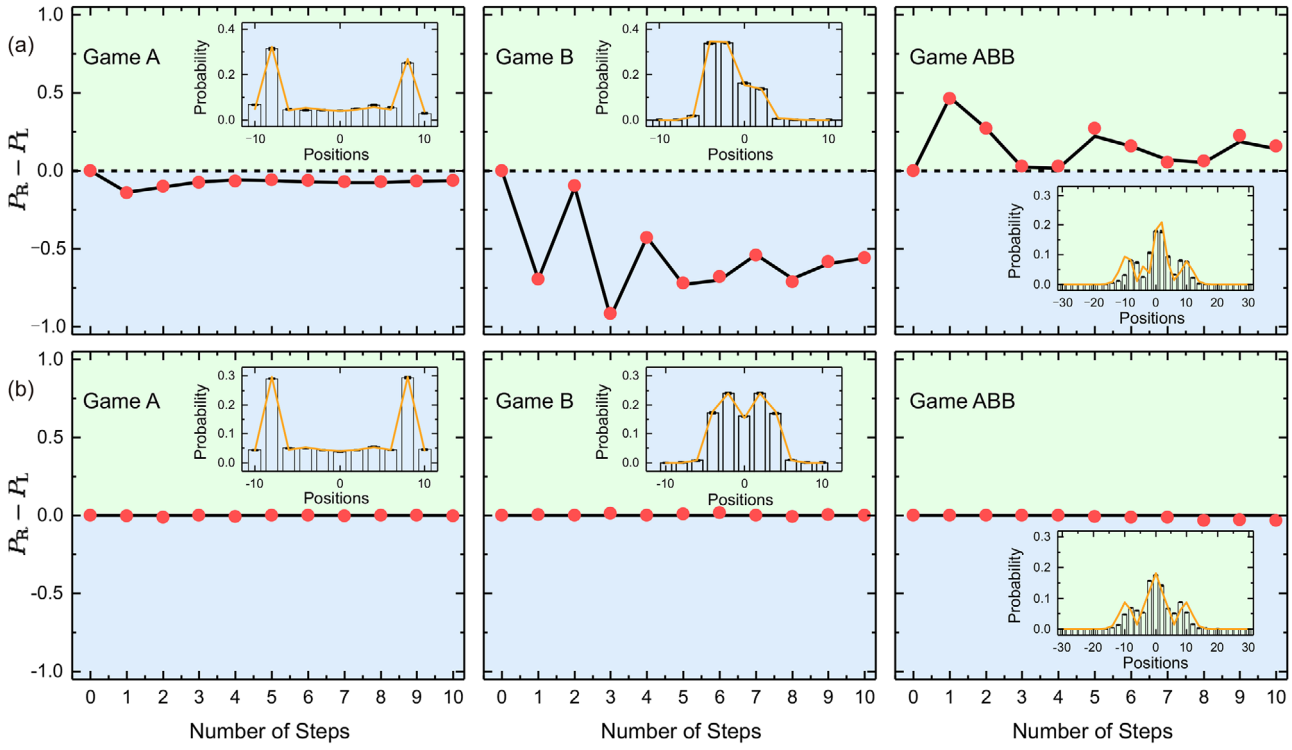

Figure 4. The measured $P_R - P_L$ versus the number of steps in the delayed-choice QWs with a) a pure coin state $(|H\rangle - i|V\rangle)/\sqrt{2}$ and b) a mixed coin state for the three games (from left to right). The solid black lines and red dots correspond to the short-range simulations and experimental results. The insets in each panel display the measured probability distributions (blue bars) and numerical simulations (solid orange lines) after a ten-step walk. Errors are estimated with consideration of the statistical noise.

the existence of the quantum Parrondo effect will be interesting (for details, see the Appendix).

4. Conclusions

We experimentally demonstrated the quantum Parrondo effect in 1D discrete-time QWs by employing multiple coin operators as different games. By measuring the mean position of the walker in its final step, we demonstrated that two losing strategies (minus the mean position) could win by playing two games in a periodic sequence, thereby exhibiting Parrondo's paradox. Furthermore, we directly extended our scheme to a version of delayed-choice QWs and found that quantum coherence plays a critical role in this quantum counterpart of Parrondo's paradox. The exact general relations between the entanglement and the quantum Parrondo effect and the coherence require additional research. We only considered the scenario of period three, and the sequence of the games is not fixed, so other sequences within a longer period may also demonstrate the Parrondo effect. Finally, quantum Parrondo games offer new opportunities and insight for alternative quantum walks.

Appendix A: Generation of Entanglement

In this section, we numerically study the coin-position entanglement in our scheme for different (dynamically) disordered QWs within a period three. The entanglement is quantified using the von Neumann entropy $S_E(\rho(t)) = -\mathrm{Tr}[\rho_C(t)\log_2\rho_C(t)]$ where $\rho_C(t) = \mathrm{Tr}[\rho(t)]$ is the reduced density matrix of the coin and $\rho(t) = |\Psi(t)\rangle\langle\Psi(t)|$ represents the global density matrix of the walker by assuming the system in a pure state. Here, $S_E = 0$ and 1 correspond to the separable and maximally entangled states, respectively. We find that the strategy ABB where the quantum Parrondo effect appears can generate the maximal entanglement in our current example within a period three (black lines in **Figure 5a**). For the other three sequences, the effect does not occur, so the entanglement generation is not optimal.

Appendix B: Quantum Coherence and the Quantum Parrondo's Paradox

To see how quantum coherence affects the quantum Parrondo effect, we investigate the stability of the Parrondo effect against the perturbation of the parameter γ in the QW by fixing the parameters α and β in R_A and R_B, which can be regarded as pure dephasing. We reconsider the games A and B with the new coin rotation operator $R'_A = R(\alpha_A, \beta_A, \gamma'_A = \gamma_A + \delta\gamma_A)$, and $R'_B = R(\alpha_B, \beta_B, \gamma'_B = \gamma_B + \delta\gamma_B)$, where $\delta\gamma_{A(B)}$ are the perturbation of the parameters $\gamma_{A(B)}$ in games A and B. Our simulation suggests that if the parameter γ'_A is still in the regime (48,53) in game A and γ'_B is in the regime (132,140), then the Parrondo effect still exists with the ABB combination of games A and B. On the other hand, if the parameters γ'_A or γ'_B are outside of this region, then the quantum Parrondo effect disappears.

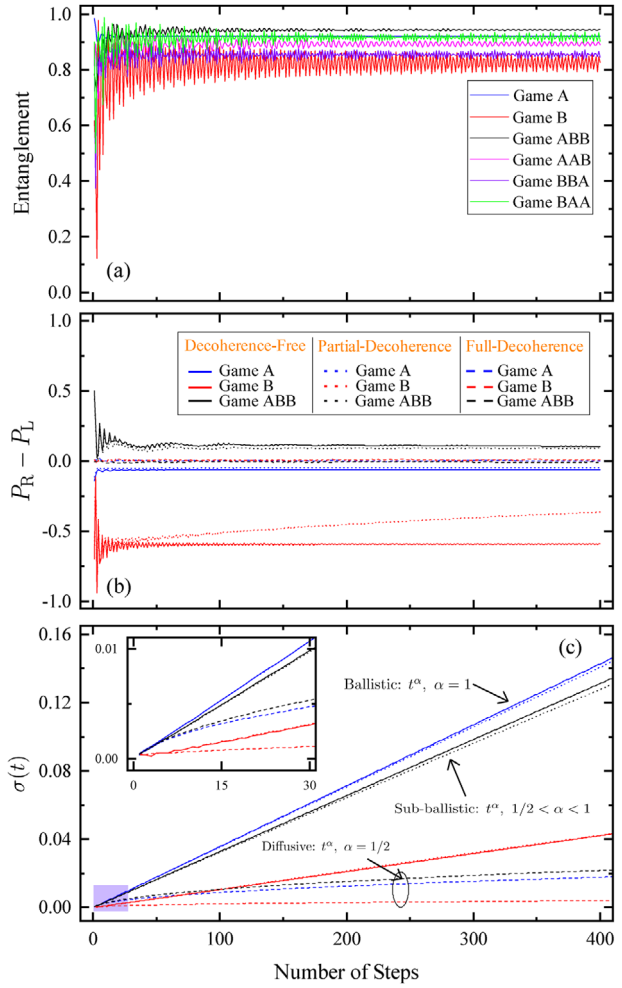

Figure 5. a) Coin-position entanglement dynamics for different games (different colors). b) $P_R - P_L$ and c) standard deviation $\sigma(t)$ as a function of the number of steps, where the solid blue (dotted), red (dotted), and black (dotted) lines correspond to games A, B, and ABB for decoherence-free (partial-decoherence), respectively. The dashed blue, red, and black lines represent the full decoherence case for games A, B, and ABB, respectively. The figure (a) demonstrates that Parrondo's games possess maximal entanglement, whereas (b) and (c) display the transition of ballistic QWs (solid curves) to diffusive CRWs (dashed curves) by adding decoherence.

To further understand the relation between decoherence and Parrondo's games, we randomly choose 400 (γ'_A, γ'_B) samples, where $\gamma'_A \in (48, 53)$ and $\gamma'_B \in (132, 140)$. For each sample i, we play the game A (B) with coin rotation operator $R'_A = R(137.2, 29.4, \gamma'_A(i))$ and $R'_B = R(149.6, 67.4, \gamma'_B(i))$, where $\gamma'_{A(B)}(i)$ is randomly chosen from the above range, to obtain the quantum state $|\Psi^i_{A(B)}(t)\rangle$. We also play the game with sequence ABB and obtain the quantum state $|\Psi^i(t)\rangle$. Then, we obtain the average state $\rho_{A(B)}(t) = \sum_{i=1}^{400} |\Psi^i_{A(B)}(t)\rangle\langle\Psi^i_{A(B)}(t)|/400$ for game A(B) and $\rho(t) = \sum_{i=1}^{400} |\Psi^i(t)\rangle\langle\Psi^i(t)|/400$ for the game with sequence ABB to mimic the effect of decoherence in the QW. Our simulation suggests that the Parrondo effect still exists with the presence of partial coherence. However, if the parameter $\gamma'_{A(B)}$ is randomly chosen from $[0, 2\pi]$, then the coherence will be completely destroyed and the effect disappears, as shown in Figure 5b.

We characterize how much residual quantum coherence is in each scenario via the transport behavior of the QW. A completely decoherent QW shows diffusive behaviors for all the games, as shown in Figure 5c. It has been shown that the sub-ballistic transport behaviors can be obtained in systems with dynamic disorder in time, including the QW with the disorder- or measurement-induced partial decoherence,[61–63] the QW with nonlinearitiy,[64–66] and the QW with time-dependent multiple-coin sequences.[67] Such sub-ballistic behaviors have been observed in many linear optical systems.[49,68] Thus, the partial-decoherence of QWs shown in Figure 5c can produce the sub-ballistic behaviors. We expect the quantum Parrondo effect in a multi-step QW with a larger period can also display such sub-ballistic behaviors although the three-period scenarios in this work approaches a ballistic behavior.

Acknowledgements

M.J. and Q.-Q.W. contributed equally to this work. This work was supported by National Key Research and Development Program of China (No. 2017YFA0304100), the National Natural Science Foundation of China (Nos. 61805228, 11474267, 11874343, 61327901, 11774335, 11821404), Key Research Program of Frontier Sciences, CAS (No. QYZDY-SSW-SLH003), Science Foundation of the CAS (No. ZDRW-XH-2019-1), the Fundamental Research Funds for the Central Universities (Nos. WK2470000026, WK2030000017, WK2470000030), the CAS Youth Innovation Promotion Association (No. 2020447), and Anhui Initiative in Quantum Information Technologies (No. AHY020100). D.A. gratefully acknowledges support by the Australian Research Council (No. DP170104984).

Conflict of Interest

The authors declare no conflict of interest.

Keywords

Parrondo's paradox, quantum optics, quantum walks

Received: November 21, 2019
Revised: March 29, 2020
Published online:

[1] J. M. R. Parrondo, presented at EEC HC&M Network on Complexity and Chaos (#ERBCHRX-CT940546), ISI, Torino, Italy, **1996**.
[2] J. M. R. Parrondo, G. P. Harmer, D. Abbott, *Phys. Rev. Lett.* **2000**, *85*, 5226.
[3] G. P. Harmer D. Abbott, *Nature* **1999**, *402*, 864.
[4] G. P. Harmer D. Abbott, *Stat. Sci.* **1999**, *14*, 206.
[5] A. P. Flitney, J. Ng, D. Abbott, *Physica A* **2002**, *314*, 35.
[6] C. F. Lee, N. F. Johnson, F. Rodriguez, L. Quiroga, *Fluct. Noise Lett.* **2002**, *2*, 293.
[7] J. Buceta, K. Lindenberg, J. M. R. Parrondo, *Phys. Rev. Lett.* **2001**, *88*, 024103.
[8] S. Khan, M. Ramzan, M. K. Khan, *Int. J. Theor. Phys.* **2010**, *49*, 31.

[9] S. Ethier J. Lee, *Markov Process. Relat. Fields* **2013**, *19*, 163.
[10] M. Li, Y.-S. Zhang, G.-C. Guo, *Fluct. Noise Lett.* **2013**, *12*, 1350024.
[11] Ł. Pawela J. Sładkowski, *Physica D* **2013**, *256*, 51.
[12] M. Pejic, *arXiv preprint* **2015**, arXiv:1503.08868.
[13] F. A. Grünbaum M. Pejic, *Lett. Math. Phys.* **2016**, *106*, 251.
[14] N. Masuda N. Konno, *Eur. Phys. J. B* **2004**, *40*, 313.
[15] D. M. Wolf, V. V. Vazirani, A. P. Arkin, *J. Theor. Biol.* **2005**, *234*, 227.
[16] F. A. Reed, *Genetics* **2007**, *176*, 1923.
[17] R. Spurgin M. Tamarkin, *J. Behav. Finance* **2005**, *6*, 15.
[18] L. Chen, C.-F. Li, M. Gong, G.-C. Guo, *Physica A* **2010**, *389*, 4071.
[19] P. Amengual, A. Allison, R. Toral, D. Abbott, *Proc. R. Soc. London, Ser. A* **2004**, *460*, 2269.
[20] F. Cannata, M. Ioffe, G. Junker, D. Nishnianidze, *J. Phys. A: Math. Gen.* **1999**, *32*, 3583.
[21] Y. Aharonov, L. Davidovich, N. Zagury, *Phys. Rev. A* **1993**, *48*, 1687.
[22] S. E. Venegas-Andraca, *Quantum Inf. Process.* **2012**, *11*, 1015.
[23] M. Santha, in *Theory and Applications of Models of Computation* (Eds: M. Agrawal, D. Du, Z. Duan, A. Li), Lecture Notes in Computer Science, vol. *4978*, Springer, Berlin, Heidelberg **2008**.
[24] R. Portugal, *Quantum Walks and Search Algorithms*, Springer, New York, NY **2013**.
[25] A. M. Childs Y. Ge, *Phys. Rev. A* **2014**, *89*, 052337.
[26] A. M. Childs, *Phys. Rev. Lett.* **2009**, *102*, 180501.
[27] A. M. Childs, D. Gosset, Z. Webb, *Science* **2013**, *339*, 791.
[28] T. Kitagawa, M. S. Rudner, E. Berg, E. Demler, *Phys. Rev. A* **2010**, *82*, 033429.
[29] T. Kitagawa, *Quantum Inf. Process.* **2012**, *11*, 1107.
[30] T. Kitagawa, M. A. Broome, A. Fedrizzi, M. S. Rudner, E. Berg, I. Kassal, A. Aspuru-Guzik, E. Demler, A. G. White, *Nat. Commun.* **2012**, *3*, 882.
[31] J. Eisert, M. Friesdorf, C. Gogolin, *Nat. Phys.* **2015**, *11*, 124.
[32] J. Lang, B. Frank, J. C. Halimeh, *Phys. Rev. Lett.* **2018**, *121*, 130603.
[33] M. Heyl, *Rep. Prog. Phys.* **2018**, *81*, 054001.
[34] X.-Y. Xu, Q.-Q. Wang, M. Heyl, J. C. Budich, W.-W. Pan, Z. Chen, M. Jan, K. Sun, J.-S. Xu, Y.-J. Han, C.-F. Li, G.-C. Guo, *Light: Sci. Appl.* **2020**, *9*, 7.
[35] J. M. R. Parrondo, J. M. Horowitz, T. Sagawa, *Nat. Phys.* **2015**, *11*, 131.
[36] S. Garnerone, *Phys. Rev. A* **2012**, *86*, 032342.
[37] A. Romanelli, *Phys. Rev. A* **2012**, *85*, 012319.
[38] A. Romanelli, R. Donangelo, R. Portugal, F. d. L. Marquezino, *Phys. Rev. A* **2014**, *90*, 022329.
[39] A. Romanelli, *Physica A* **2015**, *434*, 111.
[40] Y.-C. Jeong, C. Di Franco, H.-T. Lim, M. Kim, Y.-H. Kim, *Nat. Commun.* **2013**, *4*, 2471.
[41] A. P. Flitney, D. Abbott, N. F. Johnson, *J. Phys. A: Math. Gen.* **2004**, *37*, 7581.
[42] A. P. Flitney, *arXiv preprint* **2012**, arXiv:1209.2252.
[43] J. Rajendran C. Benjamin, *EPL* **2018**, *122*, 40004.
[44] J. Rajendran C. Benjamin, *Royal Soc. Open Sci.* **2018**, *5*, 171599.
[45] A. Schreiber, K. N. Cassemiro, V. Potoček, A. Gábris, I. Jex, C. Silberhorn, *Phys. Rev. Lett.* **2011**, *106*, 180403.
[46] N. P. Kumar, R. Balu, R. Laflamme, C. M. Chandrashekar, *Phys. Rev. A* **2018**, *97*, 012116.
[47] R. Vieira, E. P. M. Amorim, G. Rigolin, *Phys. Rev. Lett.* **2013**, *111*, 180503.
[48] R. Vieira, E. P. M. Amorim, G. Rigolin, *Phys. Rev. A* **2014**, *89*, 042307.
[49] Q.-Q. Wang, X.-Y. Xu, W.-W. Pan, K. Sun, J.-S. Xu, G. Chen, Y.-J. Han, C.-F. Li, G.-C. Guo, *Optica* **2018**, *5*, 1136.
[50] X.-Y. Xu, Q.-Q. Wang, W.-W. Pan, K. Sun, J.-S. Xu, G. Chen, J.-S. Tang, M. Gong, Y.-J. Han, C.-F. Li, G.-C. Guo, *Phys. Rev. Lett.* **2018**, *120*, 260501.
[51] L. Xiao, X. Zhan, Z. H. Bian, K. K. Wang, X. Zhang, X. P. Wang, J. Li, K. Mochizuki, D. Kim, N. Kawakami, W. Yi, H. Obuse, B. C. Sanders, P. Xue, *Nat. Phys.* **2017**, *13*, 1117.
[52] H. Obuse, J. K. Asbóth, Y. Nishimura, N. Kawakami, *Phys. Rev. B* **2015**, *92*, 045424.
[53] K. Mochizuki, D. Kim, H. Obuse, *Phys. Rev. A* **2016**, *93*, 062116.
[54] T. Machida N. Konno, *Proc. Inf. Commun. Technol.* **2010**, *2*, 226.
[55] C. Zhang, Y.-F. Huang, Z. Wang, B.-H. Liu, C.-F. Li, G.-C. Guo, *Phys. Rev. Lett.* **2015**, *115*, 260402.
[56] R. H. Hadfield, *Nat. Photonics* **2009**, *3*, 696.
[57] A. Schreiber, A. Gábris, P. P. Rohde, K. Laiho, M. Štefaňák, V. Potoček, C. Hamilton, I. Jex, C. Silberhorn, *Science* **2012**, *336*, 55.
[58] P. L. Knight, E. Roldán, J. E. Sipe, *Phys. Rev. A* **2003**, *68*, 020301.
[59] B. Sephton, A. Dudley, G. Ruffato, F. Romanato, L. Marrucci, M. Padgett, S. Goyal, F. Roux, T. Konrad, A. Forbes, *PLoS One* **2019**, *14*, e0214891.
[60] S. Dadras, A. Gresch, C. Groiseau, S. Wimberger, G. S. Summy, *Phys. Rev. Lett.* **2018**, *121*, 070402.
[61] A. Romanelli, R. Siri, V. Micenmacher, *Phys. Rev. E* **2007**, *76*, 037202.
[62] Y. Shikano, K. Chisaki, E. Segawa, N. Konno, *Phys. Rev. A* **2010**, *81*, 062129.
[63] K. Chisaki, N. Konno, E. Segawa, Y. Shikano, *Quantum Inf. Comput.* **2011**, *11*, 741.
[64] P. Ribeiro, P. Milman, R. Mosseri, *Phys. Rev. Lett.* **2004**, *93*, 190503.
[65] C. Navarrete-Benlloch, A. Pérez, E. Roldán, *Phys. Rev. A* **2007**, *75*, 062333.
[66] Y. Shikano, T. Wada, J. Horikawa, *Sci. Rep.* **2014**, *4*, 4427.
[67] A. Romanelli, *Phys. Rev. A* **2009**, *80*, 042332.
[68] A. Geraldi, A. Laneve, L. D. Bonavena, L. Sansoni, J. Ferraz, A. Fratalocchi, F. Sciarrino, A. Cuevas, P. Mataloni, *Phys. Rev. Lett.* **2019**, *123*, 140501.

